IEEE Access
Multidisciplinary ⋮ Rapid Review ⋮ Open Access Journal

Received May 11, 2020, accepted May 27, 2020, date of publication June 17, 2020, date of current version July 7, 2020.

Digital Object Identifier 10.1109/ACCESS.2020.3003231

Numerical Verification of Dielectric Contactor as Auxiliary Loads for Measuring the Multi-Port Network Parameter of Vertical Interconnection Array

BYUNGJIN BAE[1], JINGOOK KIM[1], (Senior Member, IEEE), AND KI JIN HAN[2], (Senior Member, IEEE)

[1]School of Electrical and Computer Engineering, Ulsan National Institute of Science and Technology, Ulsan 44919, South Korea
[2]Division of Electronics and Electrical Engineering, Dongguk University, Seoul 04620, South Korea

Corresponding author: Ki Jin Han (kjhan@dongguk.edu)

This work was supported by Nano-Material Technology Development Program (NRF-2016M3A7B4910430) through the National Research Foundation of Korea (NRF) funded by the Ministry of Science and Information and Communication Technology (ICT).

ABSTRACT For the accurate and reliable multi-port characterization of vertical interconnection array structures, this paper presents an indirect-contact probing method to obtain network parameters of N-port device-under-tests (DUTs) using an M-port ($N > M$) vector network analyzer (VNA) with a dielectric contactor. By utilizing the dielectric contactor as auxiliary loads for un-probed ports for vertical interconnections, multiple M-port sub-array network parameters can be correctly synthesized into the N-port network parameters through the renormalization processes. To verify the proposed method, four-port DUTs for packaging and microwave applications were characterized with two-port indirect-contact probing sub-array simulations including the dielectric contactor. Compared with two-port direct-contact probing simulations without the dielectric contactor, it was confirmed that the proposed method with the dielectric contactor provides improved accuracy in terms of the feature selective validation (FSV) method.

INDEX TERMS Dielectric contactor, de-embedding, multi-port network, port impedance, renormalization, termination load, vertical interconnection.

I. INTRODUCTION

In the design of high density packages for upcoming applications such as artificial intelligence (AI) hardware [1]–[3], an essential task is the measurement of a multitude of interconnections. For accurate characterization including electrical couplings among interconnections, multi-port vector network analyzers (VNAs) are being popularly used, but covering the entire pin counts by a single multi-port probing is usually unavailable. Instead, a feasible choice is a VNA that supports a smaller number of ports than that of the interconnections. In the typical practice, port connectors or probes should access all different partial sets of interconnections (or sub-arrays) with the other un-probed ones terminated to auxiliary loads [4], for which we can utilize passives like probing pads when measuring planar structures [5].

The associate editor coordinating the review of this manuscript and approving it for publication was Wiren Becker.

In vertical sub-array measurements, however, setting auxiliary terminations is more difficult than the planar cases since the extended passives like pads cannot be identified. Furthermore, terminating to external loads by soldering or adding connectors is not possible during successive sub-array measurements. Another difficulty in the characterization of the multi-port vertical interconnections is possible damages by the repeated contacts of many probing tips.

For the issues regarding the multi-port vertical interconnection measurements, a dielectric contactor can be a solution. In the original indirect-contact probing method [6], [7], the dielectric contactor has been devised to protect a device under test (DUT) as well as to improve accuracy. In this paper, we propose to use the dielectric contactor as auxiliary loads for un-probed ports as shown in Fig. 1, making the multi-port measurement procedure simpler. With the characterized dielectric contactor and its auxiliary loads, the multi-port measurement method including indirect-contact probing,

This work is licensed under a Creative Commons Attribution 4.0 License. For more information, see https://creativecommons.org/licenses/by/4.0/

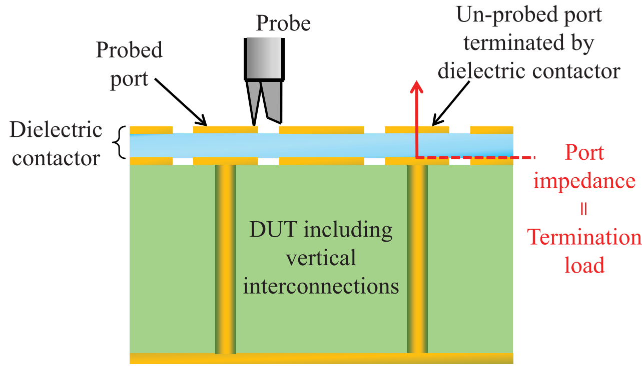

FIGURE 1. Termination of an un-probed port on a vertical interconnection using a dielectric contactor.

de-embedding of sub-arrays, renormalization, and synthesis of sub-array matrices can be established. From the numerical characterizations of three DUT examples containing four vias, the proposed method exhibits improved accuracy based on the feature selective validation (FSV) method, compared to the simple direct-contact probing method without renormalization.

II. CHARACTERIZATION OF DIELECTRIC CONTACTOR AND EXTRACTION OF AUXILIARY LOADS

This section introduces how the dielectric contactor can be characterized for the indirect-contact measurement of sub-arrays as well as for the auxiliary loads.

When measuring N-port vertical interconnection array by using an M-port ($N > M$) VNA, let K be the number of different sets of M-port sub-arrays that we should access for the completion of the N-port measurement. Once K sets of sub-arrays are determined, the proposed method to be discussed in Sec. III can be applied for any combination of N and M. Among all possible combinations, a frequent case is when M is even and N is a multiple of $M/2$. In that case,

$$K = \frac{N(2N - M)}{M^2} \tag{1}$$

different sets of M-port sub-arrays should be defined [8].

Since each indirect-contact probing measurement requires a partial network parameter matrix of the dielectric contactor for de-embedding, we need to have K different partial dielectric contactor matrices. For the kth ($k = 1, \cdots, K$) sub-array corresponding to the interconnection indices set $P_k = \{i_{k1}, \cdots, i_{kM}\}$, we can synthesize the following $2M \times 2M$ partial dielectric-contactor matrix [7]

$$\mathbf{S}_{DC,k} = \begin{pmatrix} \mathbf{S}_{DC,k}^{\text{I,I}} & \mathbf{S}_{DC,k}^{\text{I,II}} \\ \mathbf{S}_{DC,k}^{\text{II,I}} & \mathbf{S}_{DC,k}^{\text{II,II}} \end{pmatrix}, \tag{2}$$

where

$$\mathbf{S}_{DC,k}^{P,Q} = \text{diag}\left(S_{DC,pq}^{(i_{k1})}, \cdots, S_{DC,pq}^{(i_{kM})}\right),$$

and (P, p) and $(Q, q) = (\text{I}, 1)$ or $(\text{II}, 2)$. In (2), $\mathbf{S}_{DC}^{(i)} = \left\{S_{DC,pq}^{(i)}\right\}$ ($i \in P_k$) is the two-port scattering (S-) parameter matrix of the dielectric contactor part for the ith interconnect, which can be obtained in a similar way to the single interconnect case by one-port indirect- and direct-contact probing measurements on three calibration vias presented in [6], under the assumption that mutual coupling is negligible [7].

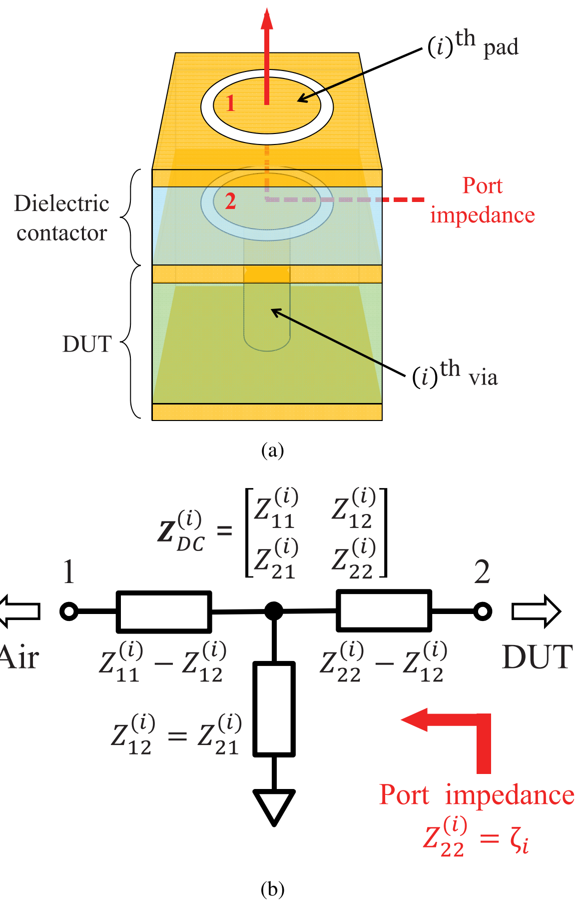

FIGURE 2. The dielectric contactor as the termination load: (a) $(i)^{\text{th}}$ pad of the dielectric contactor on the DUT (b) port impedance for $(i)^{\text{th}}$ via of the DUT in the equivalent 2-port reciprocal T-network of the dielectric contactor on the DUT.

In addition to protecting DUTs, the dielectric contactor can load un-probed DUT ports as auxiliary terminations during sub-array measurements. As illustrated in Fig. 2, the contactor mounted on the DUT has the following impedance

$$\zeta_i = Z_{22}^{(i)} \tag{3}$$

when seen from the un-probed pad of the ith interconnect. Since $Z_{22}^{(i)}$ in (3) can be found from $\mathbf{S}_{DC}^{(i)}$, no further measurement for the auxiliary load impedance is required.

The extracted dielectric contactor characteristic is used for de-embedding and renormalization during the multi-port measurement procedure, to be presented in the following section.

III. MULTI-PORT MEASUREMENT METHOD

As shown in Fig. 3, the measurement procedure is composed of indirect-contact probing measurement of sub-arrays, de-embedding of the network parameter matrices of sub-arrays,

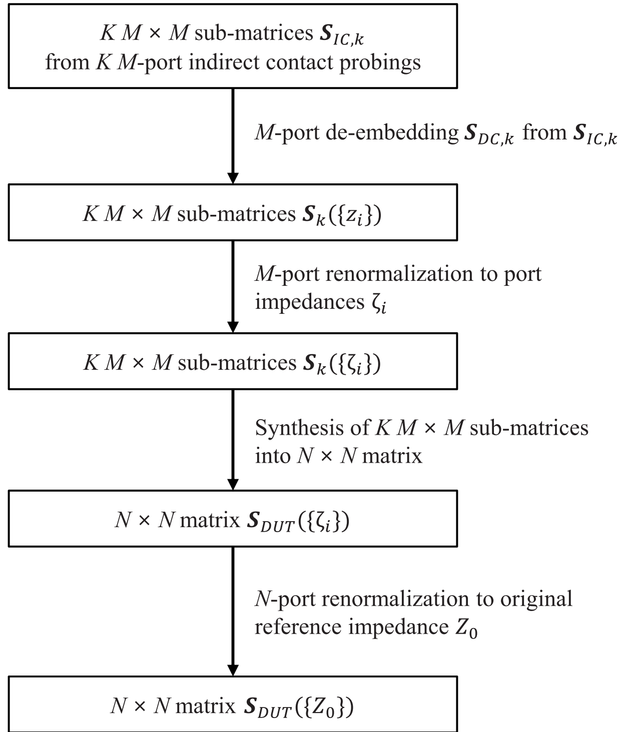

FIGURE 3. Procedure for characterization of the *N*-port network DUT with the *M*-port network analyzer using the proposed method.

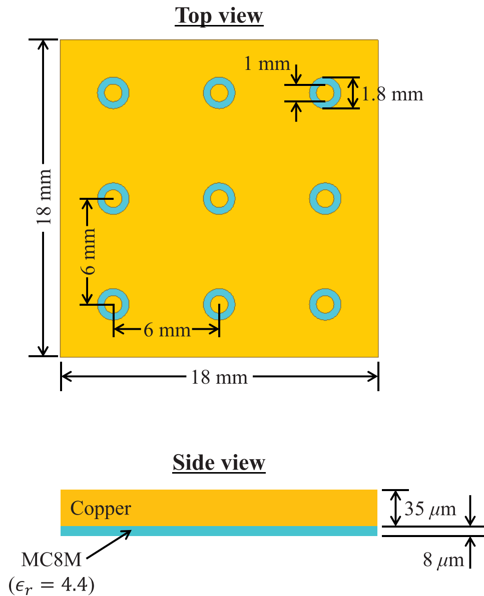

FIGURE 4. Dielectric contactor used in the numerical verifications.

renormalization of the sub-array matrices to their port impedances, construction of the entire *S*-parameter matrix, and renormalization to the reference impedances.

A. INDIRECT-CONTACT PROBING MEASUREMENT AND DE-EMBEDDING OF SUB-ARRAYS

To implement the proposed multi-port measurement method, the dielectric contactor is positioned on the DUT. Each pad of the dielectric contactor should be aligned to the pad of the corresponding DUT via, as shown in Fig. 1.

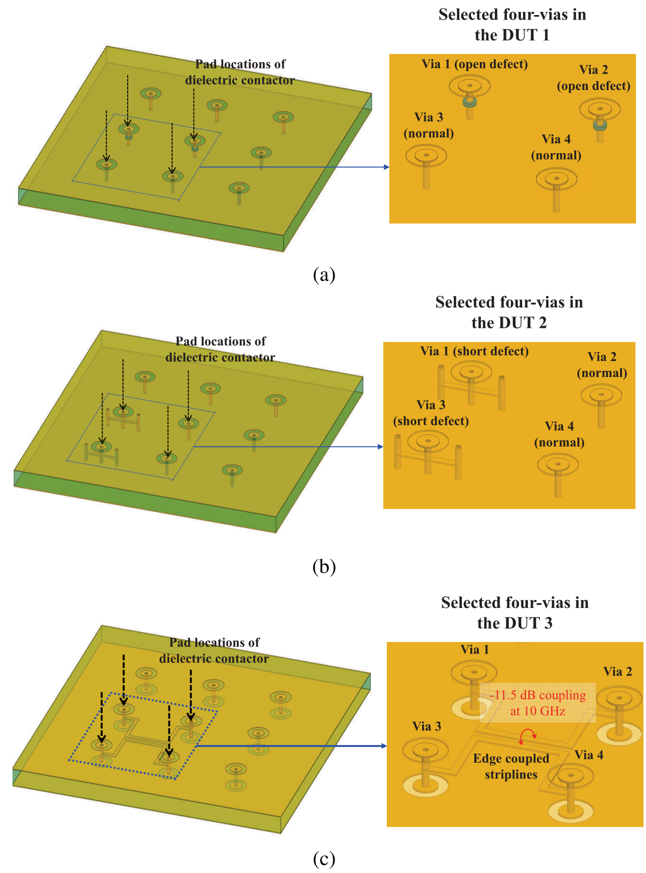

FIGURE 5. Structure of (a) DUT 1 including vias that are open-defected, (b) DUT 2 including vias that are short-defected, and (c) DUT 3 including an edge-coupled strip-line.

With the M-port network analyzer, we should apply indirect-contact probing to K sub-arrays to obtain $M \times M$ S-parameter matrices $\mathbf{S}_{IC,k}$ ($k = 1, \cdots, K$), which include the combined characteristics of the dielectric contactor and the kth sub-array. The $M \times M$ S-parameter matrix of the kth sub-array $\mathbf{S}_k$ is extracted through the M-port de-embedding of $\mathbf{S}_{DC,k}$ from $\mathbf{S}_{IC,k}$ by using the following formula [7]:

$$\mathbf{S}_k(\{z_i\}) = \left(\mathbf{S}_{DC,k}^{\text{II,II}} + \mathbf{S}_{DC,k}^{\text{II,I}} \left(\mathbf{S}_{IC,k} - \mathbf{S}_{DC,k}^{\text{I,I}}\right)^{-1} \mathbf{S}_{DC,k}^{\text{I,II}}\right)^{-1}, \quad (4)$$

where

$$z_i = \begin{cases} Z_0 & \text{if } i \in P_k \\ \zeta_i & \text{if } i \notin P_k \end{cases},$$

and P_k is the set of via indices of the kth sub-array.

B. RENORMALIZATION AND SYNTHESIS

Because of mismatches among the impedances of probed and un-probed ports, there are errors when the K sub-matrices $\mathbf{S}_k(\{z_i\})$ are simply synthesized into $N \times N$ S-parameter matrix of the entire N-port DUT. To correct the errors, the probed ports of $\mathbf{S}_k$ are M-port renormalized to the

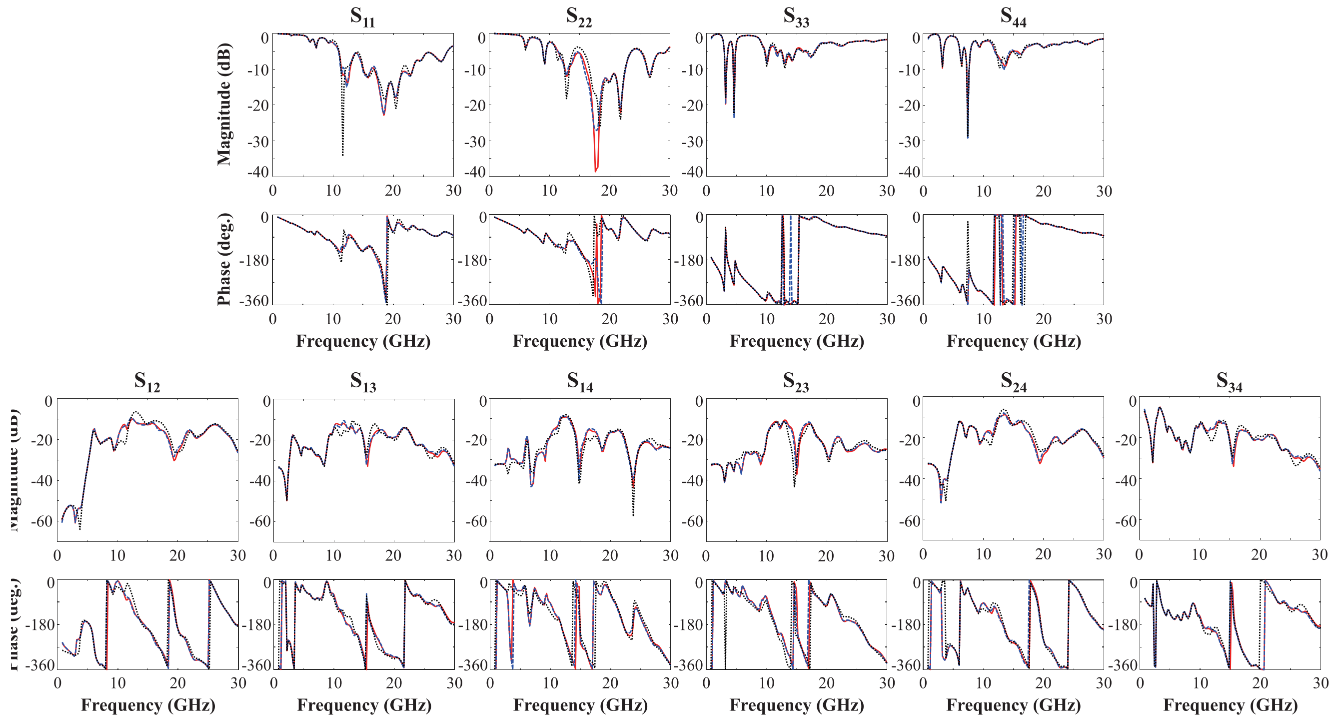

FIGURE 6. *S*-parameters of four vias with open defects (DUT 1) from the full four-port direct-contact probing simulation ($S_{DUT,\text{full direct}}$) (solid red lines), the proposed method ($S_{DUT,\text{proposed}}$) (dashed blue lines), and the two-port direct-contact probing simulations without renormalization ($S_{DUT,\text{partial direct}}$) (dotted black lines).

corresponding port impedances ζ_i by the following formula [4]:

$$\mathbf{S}_k(\{\zeta_i\}) = (\mathbf{I}_M - \mathbf{S}_k(\{z_i\}))^{-1}(\mathbf{S}_k(\{z_i\}) - \Gamma_k)(\mathbf{I}_M - \mathbf{S}_k(\{z_i\})\Gamma_k)^{-1}(\mathbf{I}_M - \mathbf{S}_k(\{z_i\})), \quad (5)$$

where $\mathbf{S}_k(\{\zeta_i\})$ is the renormalized $M \times M$ S-parameter matrices to the corresponding port impedances ζ_i, $\mathbf{I}_M$ is the $M \times M$ identity matrix, and Γ_k is an $M \times M$ diagonal matrix containing the reflection coefficients Γ_i ($i \in P_k$) of the loads ζ_i as seen from the lines of characteristic impedance Z_0.

By synthesizing K $M \times M$ sub-matrices $\mathbf{S}_k(\{\zeta_i\})$, $N \times N$ S-parameter matrix $\mathbf{S}_{DUT}(\{\zeta_i\})$ renormalized to the corresponding port impedances ζ_i ($i = 1$ to N) is obtained. Finally, another N-port renormalization to the original reference impedance Z_0 produces

$$\mathbf{S}_{DUT}(\{Z_0\}) = (\mathbf{I}_N - \mathbf{S}_{DUT}(\{\zeta_i\}))^{-1}(\mathbf{S}_{DUT}(\{\zeta_i\}) - \Gamma_N)(\mathbf{I}_N - \mathbf{S}_{DUT}(\{\zeta_i\})\Gamma_N)^{-1}(\mathbf{I}_N - \mathbf{S}_{DUT}(\{\zeta_i\})), \quad (6)$$

where $\mathbf{I}_N$ is the $N \times N$ identity matrix, and Γ_N is an $N \times N$ diagonal matrix containing the reflection coefficients Γ_i ($i = 1$ to N) of the loads Z_0 as seen from the lines of characteristic impedance ζ_i.

IV. VERIFICATION OF THE PROPOSED METHOD

In this section, we verify the proposed method by demonstrating the numerical characterization of three DUTs containing four vias using Ansys HFSS [9]. All the DUTs have four ports ($N = 4$) to the pads of four vias contained in the substrate, and two-port ($M = 2$) simulations were performed for sub-array characterizations.

As shown in Fig. 4, the dielectric contactor used in the simulations is made up of a single copper layer and a dielectric film. In the copper layer, copper pads are located at the center of the via pads of the DUT. For the data of the dielectric film, we referred to the FARADFLEX® MC8M film [10], which has a thickness of 8 μm and a dielectric constant of 4.4. When compared to the dielectric contactor used in [6], [7], possibly weaker capacitive coupling due to the lower dielectric constant of the new material has been partially compensated by its smaller thickness. In real measurements, the smaller thickness can also enhance the forward coupling and reduce the cross coupling by confirming mechanically reliable contact with the DUT.

Among the three DUTs, the first and the second structures (DUT 1 and 2) are composed of four vias, two of which are open- and short-defected as shown in Fig. 5(a) and Fig. 5(b), respectively. The two examples were selected to show that the proposed method can be used for testing multiple vias. The third DUT (DUT 3) shown in Fig. 5(c) is an edge-coupled strip-line structure, whose four ports are exposed to the top layer of the substrate through vias and pads. The coupled strip-lines were designed so that their coupling is about −11.5 dB at 10 GHz.

For quantitative verification, we compare the following two numbers $\Delta_{1(i,j)}$ and $\Delta_{2(i,j)}$ computed from simulated

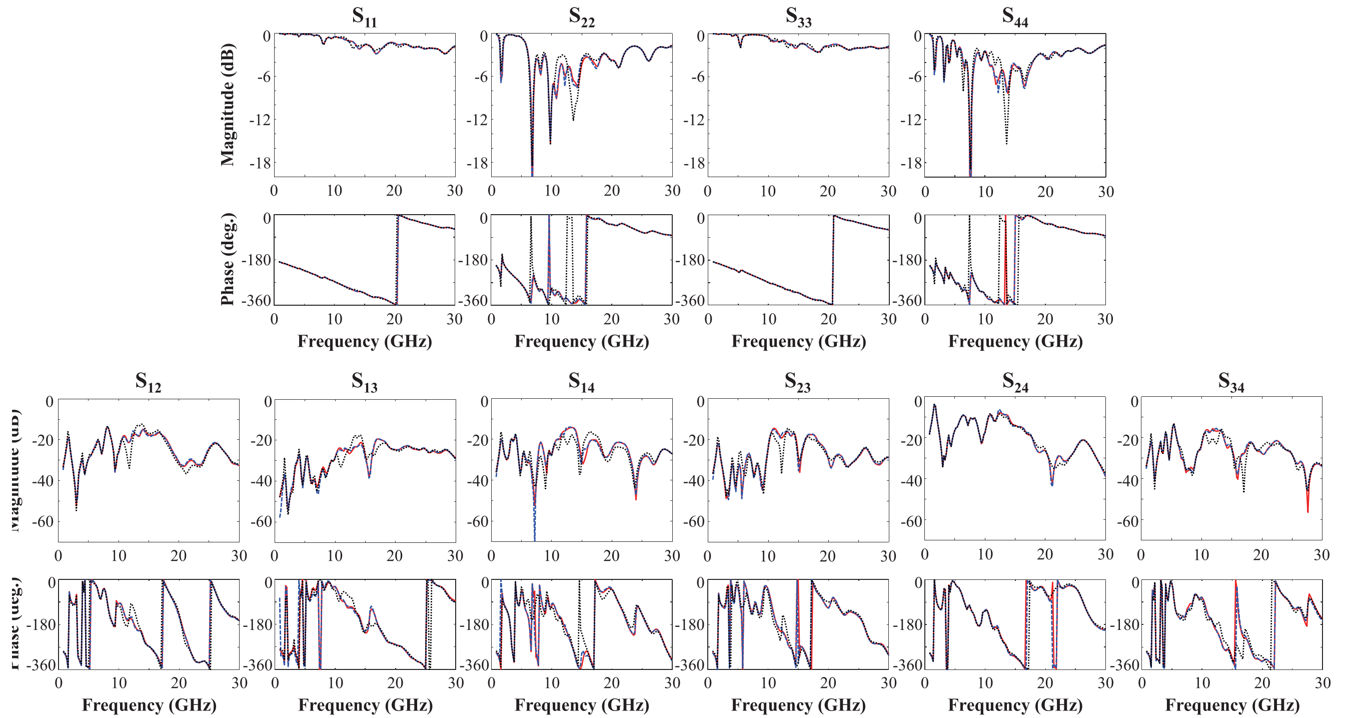

FIGURE 7. ***S*-parameters of four vias with short defects (DUT 2) from the full four-port direct-contact probing simulation ($S_{DUT,\text{full direct}}$) (solid red lines), the proposed method ($S_{DUT,\text{proposed}}$) (dashed blue lines), and the two-port direct-contact probing simulations without renormalization ($S_{DUT,\text{partial direct}}$) (dotted black lines).**

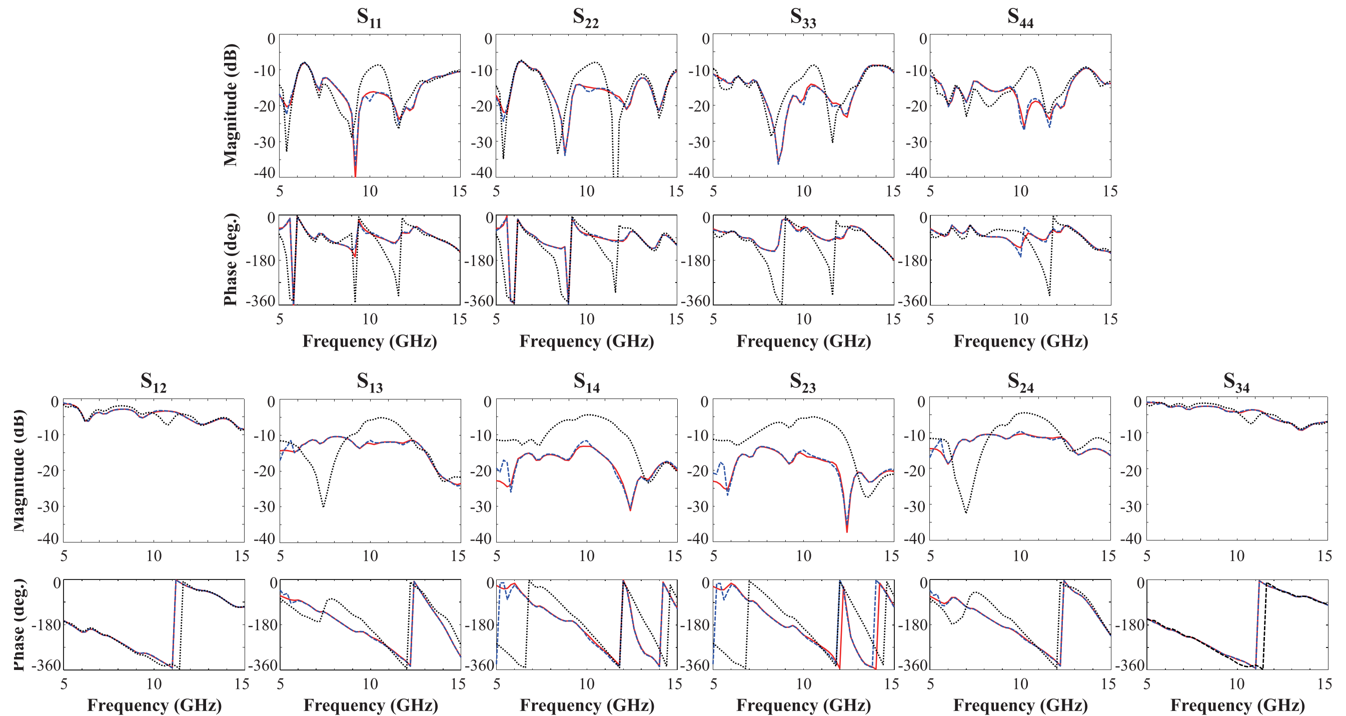

FIGURE 8. ***S*-parameters of four vias connected by coupled strip-lines (DUT 3) from the full four-port direct-contact probing simulation ($S_{DUT,\text{full direct}}$) (solid red lines), the proposed method ($S_{DUT,\text{proposed}}$) (dashed blue lines), and the two-port direct-contact probing simulations without renormalization ($S_{DUT,\text{partial direct}}$) (dotted black lines).**

data:

$$\Delta_{1(i,j)} = f\left(S_{DUT(i,j),\text{proposed}}, S_{DUT(i,j),\text{full direct}}\right)$$
$$\Delta_{2(i,j)} = f\left(S_{DUT(i,j),\text{partial direct}}, S_{DUT(i,j),\text{full direct}}\right), \quad (7)$$

where $f(x, y)$ represents any function that quantifies the difference between data sets x and y, $S_{DUT(i,j),\text{proposed}}$ is the $(i,j)^{\text{th}}$ $(i,j = 1 \text{ to } 4)$ S-parameter matrix element obtained from the proposed indirect-contact probing method discussed

in Sec. II and III, and $S_{DUT(i,j),\text{partial direct}}$ is the $(i,j)^{\text{th}}$ element obtained by synthesizing two-port simulations from direct-contact probings but without applying renormalization process. $S_{DUT(i,j),\text{full direct}}$ is the $(i,j)^{\text{th}}$ element from the full four-port direct-contact probing simulation, which can be regarded as an accurate reference since there is no error due to the contactor and the lack of renormalization.

Compared to the reference full four-port data, $S_{DUT(i,j),\text{proposed}}$ can include errors from the required calibration related to the dielectric contactor. Provided that the contactor and its auxiliary loads are correctly characterized, $S_{DUT(i,j),\text{proposed}}$ is mathematically identical to $S_{DUT(i,j),\text{full direct}}$. Although direct-contact probing is free from the calibration issue, $S_{DUT(i,j),\text{partial direct}}$ has essential errors due to the omission of the renormalization process. Without any renormalization, the matrix is crudely synthesized with the sub-matrices $\mathbf{S}_k\left(\{z_i'\}\right)$ having inconsistent reference impedances as follows:

$$z_i' = \begin{cases} Z_0 & \text{if } i \in P_k \\ \sim\infty & \text{if } i \notin P_k \end{cases}. \tag{8}$$

For the full four-port S-parameters matrix $\mathbf{S}_{DUT,\text{full direct}}$, only a single simulation is required without the dielectric contactor. The four ports in the simulation are directly set and excited through the via pads of the DUT. In the cases of synthesizing four-port S-parameters with two-port sub-array simulation data, $K = 4 \times (2 \times 4 - 2)/2^2 = 6$ simulations of two-port sub-matrices are required. In addition, the two-port simulations with the proposed method require the simulation data of the dielectric contactor for port termination and renormalization. The two ports in the simulations are set and excited on the pads of the contactor. The two-port simulations without the proposed method do not require the dielectric contactor and any port terminations, so they do not include the renormalization process. The two ports in the simulations are directly set and excited on the via pads of the DUT.

In the simulations for DUT 1 and 2, we observed their characteristics over a wide frequency range covering from 0.8 to 30 GHz because the characteristics of the vias themselves in the DUTs are important as vertical interconnections. For DUT 3, the covered frequency range is from 5 to 15 GHz because we are mainly interested in the characteristic of the coupled strip-lines in the DUT at the design frequency of 10 GHz.

The simulation results for the DUT 1, DUT 2, and DUT 3 are plotted and compared in Fig. 6, Fig. 7, and Fig. 8, respectively. In the comparisons, the reference data is the four-port S-parameters obtained from the full four-port direct-contact probing simulations. In all of the plotted graphs, it was visually verified that the four-port S-parameters obtained from the two-port sub-array simulations with the dielectric contactor are closer to the reference data than those from the two-port sub-array simulations without the dielectric contactor. Thus, we can confirm that using the dielectric contactor with a proper renormalization process ensures improved accuracy compared to a simple construction of multi-port parameters without renormalization.

TABLE 1. FSV interpretation scale [11].

FSV value (quantitative)	FSV interpretation (qualitative)
Less than 0.1	Excellent
Between 0.1 and 0.2	Very good
Between 0.2 and 0.4	Good
Between 0.4 and 0.8	Fair
Between 0.8 and 1.6	Poor
Greater than 1.6	Very poor

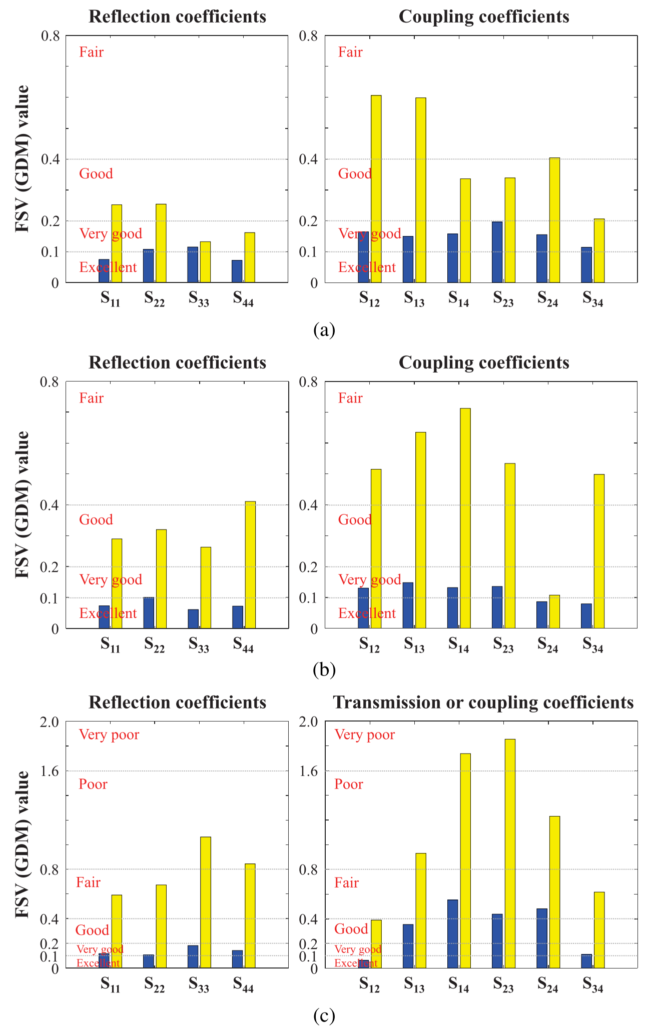

FIGURE 9. FSV (GDM) values for magnitude comparison between four-port S-parameters from the full four-port direct-contact probing simulation ($S_{DUT,\text{full direct}}$) and those from two-port simulations with the proposed method ($S_{DUT,\text{proposed}}$) (blue bars) and the two-port direct-contact probing simulations without renormalization ($S_{DUT,\text{partial direct}}$) (yellow bars). (a) DUT 1. (b) DUT 2. (c) DUT 3.

In order to quantitatively examine the effectiveness of the proposed method, the FSV method was applied to the simulated data. The FSV method is one of the candidate techniques for the quantitative validation of computational electromagnetics (CEM), particularly within electromagnetic compatibility (EMC) and signal integrity (SI) areas [11], [12]. Among measures provided by the FSV method, we used

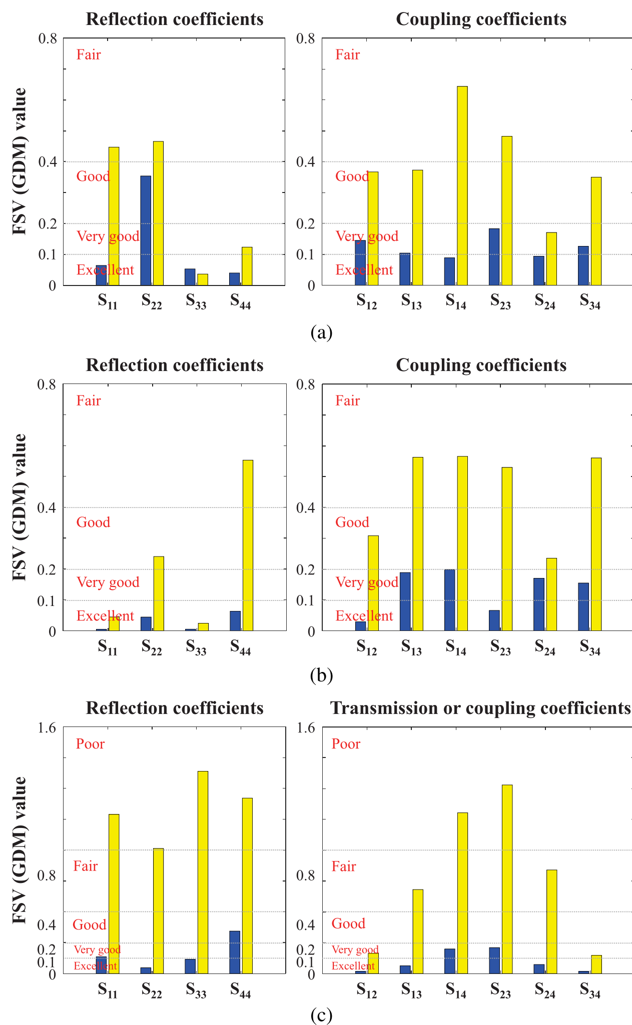

FIGURE 10. FSV (GDM) values for phase comparison between four-port *S*-parameters from the full four-port direct-contact probing simulation ($S_{DUT,\text{full direct}}$) and those from two-port simulations with the proposed method ($S_{DUT,\text{proposed}}$) (blue bars) and the two-port direct-contact probing simulations without renormalization ($S_{DUT,\text{partial direct}}$) (yellow bars). (a) DUT 1. (b) DUT 2. (c) DUT 3.

global difference measure (GDM) as the difference function f in (7) since it is a single comprehensive figure goodness-of-fit between the two data sets being compared. The GDM may be numerical or converted to a natural language descriptor such as *excellent*, *very good*, *good*, *fair*, *poor* and *very poor*, as shown in Table 1.

The GDM values calculated by using the FSV method were compared in bar graphs for the magnitude and the phase of S-parameters, as shown in Fig. 9 and Fig. 10, respectively. For the magnitude data, we used linear values without applying logarithm function. The reference data set is the four-port S-parameters ($S_{DUT,\text{full direct}}$) characterized from the full four-port direct-contact probing simulations. The data set of the first group and the second group are the four-port S-parameter synthesized from two-port simulations with the proposed method ($S_{DUT,\text{proposed}}$) and the two-port direct-contact probing simulations without renormalization ($S_{DUT,\text{partial direct}}$), respectively. All the GDM values with the proposed method in terms of both magnitude and phase are lower than those without the proposed method, except for the phase of S_{33} of DUT 1. Although the proposed method has a higher GDM value for the phase of S_{33} of DUT 1 than the direct-contact probing method without renormalization, the result is acceptable because the GDM value is in the range of *excellent*. From the results in Fig. 9 and Fig. 10, we can also confirm the effectiveness of the proposed method in the characterization of the DUTs.

V. CONCLUSION

For precise and reliable characterization of multiple vertical interconnections with a VNA having a limited number of ports, this paper proposed an indirect-contact probing measurement procedure using a dielectric contactor. In the proposed method, the dielectric contactor protects DUTs from possible contact damages by probe tips as well as are used as auxiliary terminations during the measurements of sub-arrays of interconnections. By de-embedding the characteristic of the dielectric contactor from network parameter sub-matrices including the dielectric contactor, network parameter sub-matrices for the DUT are extracted. After the de-embedding process, the multiple network parameter sub-matrices can be accurately synthesized into a full network parameter matrix with port renormalization using the previously obtained port impedances. To numerically verify the proposed method, three four-port DUTs were characterized with two-port sub-array simulations in this paper, and compared with simple direct-contact probing measurement methods. From the comparisons based on FSV method, the effectiveness of the proposed method was confirmed.

Although only four-port DUT examples were shown in this paper, the proposed method is applicable to general multi-port measurements of a multitude of package interconnections. For the realization of the presented method, a multi-port measurement system including probe cards, mechanical fixtures, stabilized automation of repeated probings, and automated processing of sub-matrices and calibration data is required. In addition, error analysis during the calibration and the renormalization processes should be performed as future work.

REFERENCES

[1] J. U. Knickerbocker, R. Budd, B. Dang, Q. Chen, E. Colgan, L. W. Hung, S. Kumar, K. W. Lee, M. Lu, J. W. Nah, R. Narayanan, K. Sakuma, V. Siu, and B. Wen, "Heterogeneous integration technology demonstrations for future healthcare, IoT, and AI computing solutions," in *Proc. IEEE 68th Electron. Compon. Technol. Conf. (ECTC)*, May 2018, pp. 1519–1528.

[2] D.-C. Hu, "Electronic packaging solutions for artificial intelligence applications (invited talk)," in *Proc. 13th Int. Microsystems, Packag., Assem. Circuits Technol. Conf. (IMPACT)*, Taipei, Taiwan, Oct. 2018, pp. 127–129.

[3] S. Mukhopadhyay, S. Yalamanchili, M. Swaminathan, Y. Long, B. Mudassar, C. S. Nair, B. H. DeProspo, H. M. Torun, M. Kathaperumal, V. Smet, and D. Kim, "Heterogeneous integration for artificial intelligence: Challenges and opportunities," *IBM J. Res. Develop.*, vol. 63, no. 6, pp. 4:1–4:1, Nov./Dec. 2019.

[4] J. Tippet and R. Speciale, "A rigorous technique for measuring the scattering matrix of a multiport device with a 2-port network analyzer," *IEEE Trans. Microw. Theory Techn.*, vol. MTT-30, no. 5, pp. 661–667, May 1982.

[5] D. G. Kam and J. Kim, "Multiport measurement method using a two-port network analyzer with remaining ports unterminated," *IEEE Microw. Wireless Compon. Lett.*, vol. 17, no. 9, pp. 694–696, Sep. 2007.

[6] J. Jeong, J. Kim, N.-W. Kang, and K. J. Han, "Indirect contact probing method for characterizing vertical interconnections in electronic packaging," *IEEE Microw. Wireless Compon. Lett.*, vol. 25, no. 1, pp. 70–72, Jan. 2015.

[7] J. Jeong, J. Kim, N.-W. Kang, and K. J. Han, "High-frequency testing of vertical interconnection array using indirect contact probing method with an improved calibration," *IEEE Trans. Compon., Packag., Manuf. Technol.*, vol. 6, no. 11, pp. 1638–1647, Nov. 2016.

[8] T. G. Ruttan, B. Grossman, A. Ferrero, V. Teppati, and J. Martens, "Multiport VNA measurements," *IEEE Microw. Mag.*, vol. 9, no. 3, pp. 56–69, Jun. 2008.

[9] *HFSS Ver. 16.2*, Ansys, Inc., Canonsburg, PA, USA, 2015. [Online]. Available: https://www.ansys.com/products/electronics/ansys-hfss

[10] *FARADFLEX*, MCMseries datasheet, 2017.

[11] A. Duffy, A. Martin, G. Antonini, A. Orlandi, and C. Ritota, "The feature selective validation (FSV) method," in *Proc. Int. Symp. Electromagn. Compat. (EMC)*, Chicago, IL, USA, vol. 1, 2005, pp. 272–277.

[12] *IEEE Recommended Practice for Validation of Computational Electromagnetics Computer Modeling and Simulations*, IEEE Standard 1597.2-2010, Feb. 2011, pp. 1–124.

BYUNGJIN BAE received the B.S. degree in electrical engineering from the Ulsan National Institute of Science and Technology (UNIST), Ulsan, South Korea, in 2017, where he is currently pursuing the Ph.D. degree. His current research interests include electrostatic discharge (ESD) and electromagnetic compatibility (EMC).

JINGOOK KIM (Senior Member, IEEE) received the B.S., M.S., and Ph.D. degrees in electrical engineering from the Korea Advanced Institute of Science and Technology, Daejeon, South Korea, in 2000, 2002, and 2006, respectively. From 2006 to 2008, he was with the Memory Division, DRAM Design Team, Samsung Electronics, Hwasung, South Korea, as a Senior Engineer. From January 2009 to July 2011, he worked with the EMC Laboratory, Missouri University of Science and Technology, Missouri, USA, as a Postdoctoral Fellow. In July 2011, he joined the Ulsan National Institute of Science and Technology (UNIST), Ulsan, South Korea, where he is currently an Associate Professor. His current research interests include analog circuit design, electromagnetic compatibility (EMC), and electrostatic discharge (ESD).

KI JIN HAN (Senior Member, IEEE) received the B.S. and M.S. degrees in electrical engineering from Seoul National University, Seoul, South Korea, in 1998 and 2000, respectively, and the Ph.D. degree in electrical and computer engineering from the Georgia Institute of Technology, Atlanta, GA, USA, in 2009.

He was with the System Research and Development Laboratory, LG Precision Company, Ltd., Yongin, South Korea, from 2000 to 2005. From 2009 to 2011, he was with the IBM Thomas J. Watson Research Center, Yorktown Heights, NY, USA, as a Postdoctoral Researcher. He is currently an Associate Professor with the Division of Electronics and Electrical Engineering, Dongguk University, Seoul. His current research interests include computational electromagnetics, electromagnetic compatibility and reliability for power electronics, signal/power integrity for high-speed digital design, and the electrical modeling of electronic packaging and interconnections.

Dr. Han was a recipient of the Samsung Scholarship for Graduate Study, in 2005, and the Best Paper Award of the IEEE Transactions on Components, Packaging, and Manufacturing Technology (TCPMT), in 2016. He served as the Technical Program Committee Chair of the IEEE Electrical Design of Advanced Packaging and Systems Symposium, in 2015. He has been serving as an Associate Editor for the IEEE TCPMT, since 2018.